The phase behaviour and gelation of a rod-like polymer in solution and implications for microcellular foam morphology

C. L. Jackson* and M. T. Shaw
The Institute of Materials Science, The University of Connecticut, Storrs, CT 06268, USA
(Received 29 June 1989; accepted 26 July 1989)

The phase separation and gelation of the rod-like macromolecule, poly(γ-benzyl-L-glutamate), were studied in an effort to understand the mechanism by which microcellular materials are made via thermally induced phase separation processes. Previous workers have studied similarly prepared materials from molecules which exist as random coils in solution. The microcellular materials were formed by lowering the solution temperature until phase separation and solvent freezing occurred. The solvent was removed by vacuum sublimation. An emphasis was placed on dilute isotropic solutions (<5 wt%) which yield low-density materials or 'foams'. Both one- (e.g. benzene) and two-component (e.g. dioxane/water) solvent systems were employed. The morphology produced by liquid–liquid phase separation and gelation was an open-celled, fibrous structure, which resembles a three-dimensional lattice. The cell diameters were in the range of 1–10 μm and the fibres which comprise the struts were 0.2 to 2.0 μm thick. Various experimental observations are discussed in terms of the theories and proposed mechanisms of phase separation in solutions of rod-like macromolecules. Calculations of the spinodal for the Flory theory of rod-like particles were also made to assess the possibility of placing the isotropic solutions into an unstable region.

(Keywords: liquid crystal polymer; foam; microcellular; gel; phase behaviour; poly(γ-benzyl-L-glutamate))

INTRODUCTION

The liquid–liquid phase separation of polymer solutions has been used to produce membranes[1], filled microporous polymers[2] and microcellular materials or foams[2–6]. The phase separation may be induced by adding a non-solvent or by lowering the temperature of the solution. The solvent is removed by extraction or sublimation. The solution behaviour of the polymer is of key importance to the resulting foam morphology. Amorphous polymers such as atactic polystyrene in cyclohexane have produced highly interconnected structures for which a spinodal decomposition mechanism has been suggested[3]. In combination with liquid–liquid phase separation, semi-crystalline polymers often gel, because physical crosslinks can form via crystallites. Poly(4-methyl-1-pentene) in 1,2-diphenylmethane[4] and isotactic polystyrene in nitrobenzene[6] are examples of gels from which microcellular foams have been prepared.

Foams prepared from solutions are unique because of the open cell structure and small cell diameter (0.1–20 μm) relative to closed cell foams of similar density made by conventional thermoplastic foam extrusion (100–200 μm). Prior to the work we will present in this article, the emphasis has been on low-density foams (<0.1 g/cm^3) made from dilute solutions of random coil polymers[3–6]. These new materials have the potential for many applications such as filters, controlled release media, catalytic substrates, artificial skin and blood vessels and three-dimensional reinforcements for composites. The combination of low density, small cell size and high surface to volume ratio in a material has not been exploited commercially except in the higher density form of very thin membrane structures.

A comparison of random coil polymers and rigid-rod polymers in solution illustrates that many unique properties are afforded by the anisotropic molecular shape. Dilute solution properties are affected by the larger radius of gyration, R_G, of the elongated rod form[7], and the relation $R_G \propto M^{\nu}$ applies, with $\nu = 1.0$. For flexible polymers $\nu \approx 0.6$. Lower critical overlap concentrations[8], larger intrinsic viscosities, larger relaxation times and smaller diffusion constants[7] are thus observed in rigid-rod solutions. In solutions of sufficiently high concentration, rigid-rod polymers can form liquid crystals, and they are also called lyotropic liquid crystal polymers (LCPs). In the solid-state, LCPs have provided excellent mechanical properties in fibres and composite materials[9,10]. If microcellular foams could be made from rigid-rod polymers, they may offer such features as superior mechanical properties, dimensional stability and solvent resistance due to the highly crystalline nature of the solid polymer. Controlled anisotropic structures may be possible by pre-ordering solutions of rigid-rod polymers in the liquid crystal state, using electric or magnetic fields, which may further enhance mechanical properties. A lower density foam may also be possible due to the lower overlap concentration in solution (for rods and coils of equivalent molecular weight).

The present study includes the preparation and characterization of microcellular materials which are formed from rigid-rod solutions via phase separation processes. To the best of our knowledge, this is the first example of a synthetic foam from a solution of an LCP prepared by this method. Poly(γ-benzyl-L-glutamate) (PBLG) was the polymer chosen for this work, primarily due to

* Present address and to whom correspondence should be addressed: Polymers Division, National Institute of Standards and Technology, Gaithersburg, MD 20899, USA

0032-3861/90/061070-15

solubility in common organic solvents[11,12] and degree of chain rigidity[13]. The rod-like shape of the polymer in both the solid state and in solution is the result of an α-helix stabilized by hydrogen bonds[14]. Previous transmission electron microscopy experiments to visualize precipitates of PBLG showed twisted, rope-like fibrils interconnected into a network in two dimensions[15,16]. In this work we show that three-dimensional macroscopic gels and foams having similar unique structures can be produced.

The study of foams made from lyotropic LCPs also gives insight into the phase behaviour of rigid rods in the wide biphasic region, because the foam may be regarded as a relic of the phase decomposition process. Thermoreversible gelation has been observed upon cooling solutions of rod-like polymers[17–22], and the relationship between gelation and the miscibility gap is not yet clear. This network formation may be a result of spinodal decomposition[17] or a crystal–solvate phase which is a result of nucleation and growth[20–22]. The relationship between liquid–liquid phase separation and gelation for flexible polymers is also not thoroughly understood[23,24].

We chose to study solvents which could be readily removed from the frozen solution by vacuum sublimation. Solvents to be discussed include dioxane, 1,4-dichlorobenzene, naphthalene, 1,2-dichloroethane, and benzene. The influence of miscible cosolvent systems was also investigated, where a small amount of non-solvent for the polymer is added to adjust the phase equilibria. This method has been successfully employed for foams made from polystyrene solutions[3]. Cosolvent systems studied include dioxane/isopropyl alcohol and dioxane/water. Foams prepared from liquid–liquid phase separation processes were anticipated to produce the small-cell-size materials of interest and were the central focus of this work. The emphasis was on low density foams ($<0.1\,g/cm^3$) made from dilute isotropic solutions.

EXPERIMENTAL

Materials

Poly(γ-benzyl-L-glutamate) (PBLG) samples were purchased from Sigma Chemical Company. Two designations were used for the polymer molecular weights; low (PBLGL; $M_v = 6.6 \times 10^4$ g/mol) and high (PBLG; $M_v = 1.9 \times 10^5$ g/mol). For most experiments the highest molecular weight polymer was used. The solvents were all h.p.l.c. grade or Gold Label grade from Aldrich Chemical Company, except naphthalene, which was reagent grade from Baker Chemical Company. The dioxane was dried over sodium sulphate, filtered and stored over 3 Å molecular sieves.

Solution studies

All solutions were prepared on a weight basis, unless otherwise specified. The density of bulk PBLG is $1.296\,g/cm^3$. For PBLG solutions in which a cosolvent was used, the polymer was first dissolved in the good solvent for 1–2 days prior to slow addition of the non-solvent. Solvents which were liquid at room temperature were warmed to 50°C to facilitate dissolution. Solvents which were solid at room temperature were prepared by weighing the solid solvent and polymer into a small vial, degassing under vacuum and flame sealing with a torch. These solutions were heated to 100–120°C to dissolve the polymer.

Differential scanning calorimetry (d.s.c.) results were obtained on a Perkin–Elmer DSC 7. D.s.c. pans specially designed for liquids were used, and sample weights were 30–70 mg. The pans were weighed before and after testing to assure that solvent was not lost.

Cloud points of the solutions were determined by either of two methods. The first involved a phase characterization apparatus (PCA) designed for the Rheometrics System IV[25]. In this set-up, a fibre optics light source and a detector were used to measure backscattered light from a solution sealed in a glass vial. The temperature of the solution was controlled by the System IV oven, which has a temperature range of −150 to 400°C. The dynamic motor was used for most experiments to turn the vial in an oscillating fashion using the 'cure mode' of the System IV. The oscillation provided a constant mixing for the solution. A cooling rate of 1°C/min was used and a correction for the temperature difference between the vial and thermocouple was made using a calibration curve of pure solvents.

The PCA was able to distinguish between a clear solution, a cloudy solution, and a crystalline solid by the intensity of backscattered light. The geometry of the set up also allowed the detection of gelation. These effects are illustrated schematically in *Figure 1*. The intensity of backscattered light from the clear solution is greater than that for the cloudy solution due to the reflection of the incident beam off the meniscus of the solution in the vial. In the case of the crystalline solid, the beam reflects off the outside of the vial into the detector and produces an even greater intensity than the clear solution. The gelled system produces large amplitude oscillations, which may also shift in intensity if the gel is cloudy.

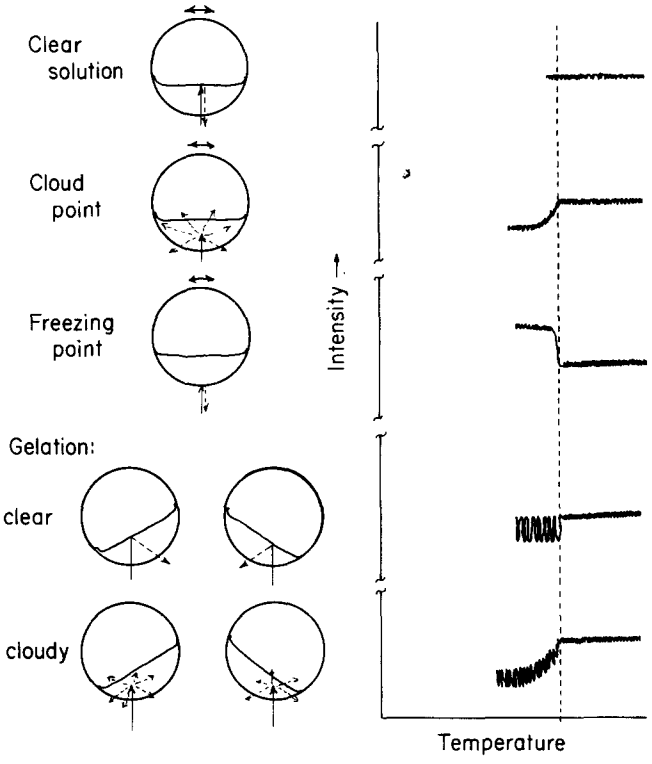

Figure 1 Schematic diagram of phase characterization apparatus data showing relative intensity of light backscattered from solution *versus* temperature for various experimental conditions

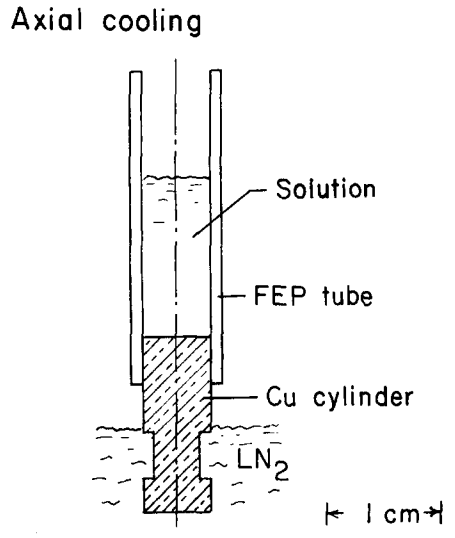

Figure 2 Design of foam mould for uniaxial quench

Analysis of cloud points with the PCA allowed only one sample to be run at a time and used large quantities of liquid nitrogen at the slow cooling rates necessary to obtain equilibrium data. Thus, a second method was used. This method employed a programmable bath at a cooling rate of 0.1°C/min. Quiescent cloud points were visually detected on 0.25 g of solution, flame-sealed in a 5 mm n.m.r. tube.

Gelation studies

Rheological measurements were conducted using a Rheometrics System IV fluids motor and a couette geometry. The couette fixtures, containing 20–25 ml of solution, were immersed in a cooling bath of ethylene glycol/water (50/50). The temperature of the test solution normally read within 1°C of the bath temperature. A comparison of the two served as a crude thermal analysis method, allowing detection of solvent freezing. The materials studied were somewhat complex in that clouding, gelation and freezing all occurred over a small temperature range. Thus, the detection of heat evolution during crystallization was useful.

Evaporation of solvent from the test solutions was minimized by constructing a split Plexiglass cover for the top of the bath with a hole just large enough for the transducer shaft to fit through. In addition, the atmosphere above the bath was saturated with a solvent-soaked ring of filter paper placed on the rim of the cup. Solutions could be maintained in the bath for over 6 h at 27°C with no change in viscosity when solvent was added to the filter paper once per hour. Repeated cooling and heating cycles of the solutions also produced no change in the results. The dynamic storage modulus, G', and loss modulus, G'' were monitored as a function of temperature at a frequency of 1 Hz. Both cooling and heating cycles were studied at rates of 0.125–0.5°C/min. A rate of 0.25°C/min was used, however, for most experiments. Small strains (1.0–3.0%) were employed to minimize disruption of the gelation process.

Foam preparation

The foams were initially synthesized using a small scale version of the mould described by Aubert and Clough[3] which provides uniaxial cooling of the solution during the quench. A schematic diagram of this mould is shown in *Figure 2*. The bottom of the mould was a solid copper cylinder approximately 1 cm long and 6 mm in diameter, with a notch in the base. The copper base was fitted with a fluorinated ethylene polymer (PEP) tube to hold the solution. The notch was used along with a slotted clamp to allow rapid removal of the copper base from the tube after the sample was frozen. A slightly larger version of this design (1.8 cm in diameter) was also constructed to prepare larger foams.

The solution was loaded into the mould to a height of about 1 cm. The copper base was submerged in the cooling fluid, usually liquid nitrogen, until the solution was completely frozen. This process took about two minutes using liquid nitrogen. (This corresponds to a cooling rate of $\simeq$100°C/min.) Phase separation (cloudiness) and solvent freezing could be observed through the FEP tube. The copper base was then removed from the tube using the notch and the frozen sample was pushed out of the mould into an insulated, pre-cooled freeze-drying vessel. The sample was placed on a vacuum line at $\leqslant$50 mTorr for 3–12 h, depending on the size of the sample. For the lower melting solvents, active cooling of the vacuum vessel was provided with dry ice/acetone baths, and much longer freeze-drying times were employed.

Foam characterization

Methods used for foam characterization included bulk density measurements, scanning electron microscopy (SEM), optical microscopy, wide angle X-ray diffraction (WAXS) and modulus measurements.

The measurement of bulk foam density on samples prepared in the small mould was very difficult because the samples typically weighed less than 10 mg. Therefore most foams are referred to by their original solution concentration. As reported by Aubert and Clough[3], some shrinkage of the foam was observed during the freezing and the freeze-drying steps, depending on the specifics of the process such as the strength of vacuum in freeze drying. To estimate the shrinkage occurring at various polymer concentrations, a series of foams was prepared in the large cylindrical foam mould ($d = 1.8$ cm) using one of the most studied solvent systems: dioxane/water. All members of this series weighed >15 mg. In the range of 1–4% PBLG, the shrinkage was about 60%. At solution concentrations of 0.5%, extreme shrinkage (>300%) was observed and the density measurement was only an estimate because the cylindrical geometry was not well preserved. For the 2% PBLG solution, the foam density, along with the 95% confidence interval, was calculated to be 0.032 ± 0.0029 g/cm^3.

The foam morphology was examined on an Amray Model 1000A SEM. The cylindrical foams were generally cut in half along the z direction and examined from bottom to top to assess the effect of quench rate on foam morphology. The cut surface for microscopy and mechanical tests was prepared using a microtome blade which oscillated horizontally at a rate of 43 strokes/s. The length of the stroke was 1 mm. The samples were glued securely to a SEM stub or other piece of metal with Duco cement, silver painted along each side, outgassed overnight under high vacuum (10^{-7} Torr), and sputter coated with a Au/Pd layer approximately 100 Å thick.

Optical microscopy was performed on slices of the foam embedded in epoxy resin and sectioned on an ultramicrotome to a thickness of 4 μm. The embedding medium, Polybed 812 (Polysciences, Inc.), was prepared according to the manufacturer's instructions. The samples were prepared in polyethylene capsules designed to fit in a microtome chuck. The resin was degassed under vacuum, the foam slices were added, and the vacuum was continued to allow air in the foam to be replaced by resin, before curing the epoxy at 60°C overnight. The sign of the birefringence was determined using a first-order red plate by comparison to fibres of known sign of birefringence.

WAXS was performed on a Rigaku Rotating Anode at 40 kV and 260 mA using Cu–Kα ($\lambda = 1.54$ Å) radiation. The film to sample distance was 60 mm. Exposure times of 0.5 to 3 h were used. Thin slices of the foam, prepared with the vibrating microtome described earlier, were cut into 2 mm strips with a sharp blade. The strips were stretched to induce orientation, then mounted on a wire frame and secured at both ends to prevent relaxation. Unstretched foam samples were also examined.

Modulus measurements on the foam were made in tension/compression using the linear motor on the Rheometrics System IV with the parallel plate fixtures[26]. Foam samples varying from 1–4 mm in thickness were cut into rectangular pieces and glued to the plates to correct for any minor non-parallelism of the cut surface. Various rectangular sizes were tested to check for the 'constrained cylinder' effect, which occurs in solids when the diameter to height ratio is large and the ends of the specimen are constrained[27]. Such effects were not observed for the foams, which are fairly low-density and highly compressible. Strains of less than 1% were used in non-destructive tests of the modulus, at a frequency of 1 Hz. More specific details of the modulus tests are given elsewhere[26].

RESULTS AND DISCUSSION

The study of the phase behaviour of rod-like polymers at concentrations well below the predicted isotropic to liquid crystal transition was the main focus of this work. Of particular interest was the dynamics (or mechanism) of phase separation as the temperature is lowered into the wide biphasic region. In the first section of the results, a brief review of the Flory theory of the phase behaviour of rod-like particles will be given, along with our calculation of the spinodal curve as it relates to an isotropic solution of rods.

The experimental work is then presented, according to whether the phase separation was determined to be liquid–liquid or liquid–solid. This determination was made by studying solutions of PBLG as a function of temperature for evidence of liquid–liquid phase separation, or a cloudy appearance, prior to solvent freezing. Thermoreversible gelation has also been observed in the wide biphasic region and may complicate the phase equilibrium behaviour[13]; we also report our findings in this area. The foam morphology obtained from each type of phase separation is then summarized, followed by a discussion of the mechanism of liquid–liquid phase separation in these systems, based on the experimental results. The primary focus was on liquid–liquid phase separation, which occurs on a microscopic scale and is of basic theoretical and practical interest. The discussion on liquid–solid phase separation is given for contrast and clarity.

Theory of phase equilibria of rod-like particles

A number of theoretical approaches have successfully predicted the self-ordering of rod-like particles above a certain critical concentration. The two which are most noted are the virial expansion method of Onsager[28] and an adaptation[29] to the Flory lattice treatment for flexible polymers. Subsequent extensions and criticisms have been given to both theories[30,31], however, very little attention has been paid to the mechanism, or dynamics of the phase separation process. This is in distinct contrast to solutions and blends of flexible polymers, where the mechanism of phase separation (nucleation and growth or spinodal decomposition) is commonly studied.

The complexity of molecular interactions of rod-like polymers, such as the excluded volume, entanglements and hydrodynamics, makes an accurate description of the dynamics difficult. In particular, the translation and diffusion of a rod-like polymer is strongly influenced by the proximity of other rods. Thus, the dynamics differ greatly depending on the concentration of the solution[7]. For the semi-dilute or concentrated isotropic solutions of interest in this work, a new kinetic equation for the structure factor has been proposed by Doi[32] which is applicable in the single phase isotropic region. An extension to the phase-separated solution which forms in the wide biphasic region upon lowering the temperature has not yet been made.

A few researchers have simply attempted to extend the principles of the dynamics of liquid–liquid phase equilibria in flexible polymers to rigid-rod systems. These extensions have used the Flory theory of rod-like particles[29], because it is applicable over a broader concentration range and includes the temperature dependence in the interaction parameter, χ, well known to polymer scientists. We have chosen the Flory theory for our spinodal calculations for similar reasons, although we are aware of the limitations of the theory, which will be discussed. In the Flory theory, one free energy function describes the isotropic phase and is termed 'disordered', and a second free energy function describes the anisotropic liquid crystal phase and is termed 'ordered'. The spinodal curve is calculated by setting the second derivative of the free energy function equal to zero and solving for χ_{sp}.

For the dilute isotropic region of interest in this work, the calculation of the spinodal of Flory's disordered free energy function for rods is of interest. We have made such a calculation for rods with an axial ratio of 100, shown in *Figure 3* as the evenly spaced dashed curve. This curve is given along with the binodal curve for a solution of rods given by Flory, shown as the solid curve. The critical volume fraction at which the isotropic–nematic transition is predicted to occur for this axial ratio is 0.078, which is indicated by a vertical mark on the disordered spinodal curve. The continuation of the disordered spinodal curve beyond the critical concentration is included as a lighter dashed line, to indicate the behaviour of this function. If the theory is strictly adhered to, a rather large gap exists between the binodal and the spinodal curves at low polymer concentrations.

A similar calculation of the spinodal of Flory's ordered free energy function for rods has been made by Wee and Miller[33]. This result is shown as the uneven dashed curve

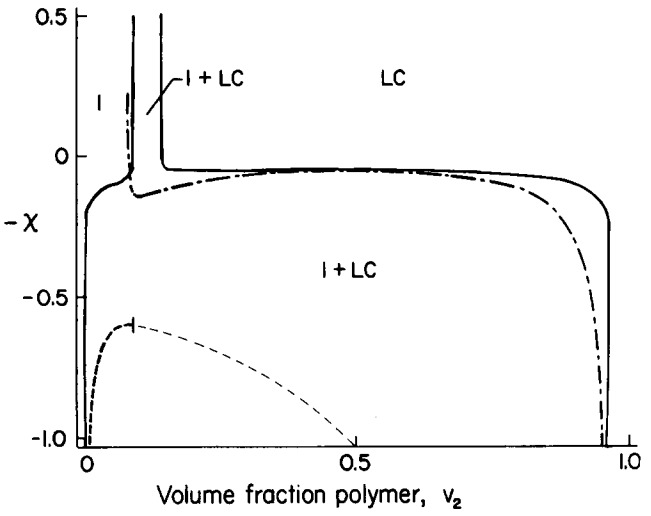

Figure 3 Calculation of the spinodal curve for the Flory theory of rod-like particles for rods of axial ratio, $x=100$, where I = isotropic and LC = liquid crystalline: the even and uneven dashed lines are the spinodals of the disordered (this work) and ordered (ref. 33) free energy functions, respectively, and the solid curve is the binodal (ref. 29)

in *Figure 3*. In the ordered region, the spinodal lies close to the binodal curve, and the unstable region appears to be quite accessible over a large concentration range. The sharp upturn of the spinodal close to the critical concentration may be a result of the proximity to the boundary condition inherent in the derivation.

The discontinuous nature of the spinodal shown in *Figure 3*, which is a result of the two free energy functions given by the Flory theory, may not be representative of the behaviour of rod-like polymers in the vicinity of the narrow biphasic region and at lower concentrations. Indeed, a primary weakness of the Flory theory is the artificiality of the lattice model at low polymer concentration. Because this is the region of interest in this work, the application of the theory is suspect. It is hoped that the presentation of the problem may serve as a basis for future theoretical work on the dynamics of phase separation and spinodal decomposition of solutions of rod-like polymers.

Liquid–liquid phase separation

Phase behaviour. The cloud point was interpreted as the boundary of the wide biphasic region, where a dilute isotropic solution coexists with a concentrated LC solution, as predicted by Flory[29]. To simplify the eventual production of microcellular foams, an emphasis was placed on solvents which readily sublime. Liquid–liquid phase separation was observed upon cooling solutions of PBLG in 1,2-dichloroethane, dioxane/isopropyl alcohol (70/30), dioxane/water and benzene. However, the most extensive work was done on the benzene and dioxane/water solutions and gels, because foams were most successfully prepared from these solvents. Examples of PCA traces obtained for each solvent system are shown in *Figure 4*. Using the criteria set forth in *Figure 1*, it was deduced that gelation occurred in conjunction with liquid–liquid phase separation, and rheological measurements were made on some systems.

The phase diagram for 1–9% PBLGL in 1,2-dichloroethane[34] is shown in *Figure 5*. Solutions in this concentration range were all isotropic at room temperature. At polymer concentrations exceeding 3%, a liquid–liquid transition did occur before solvent freezing; for the 5% PBLGL solution this was approximately −30°C. The low melting point of this solvent (−35°C) however, made foam synthesis difficult. Although pure solvent was successfully sublimed, using active cooling to keep the sample frozen, the frozen polymer solutions tended to melt on the surface during transfer to the vacuum vessel. Attempts to process foams from polymer solutions in glass tubes also failed in most cases.

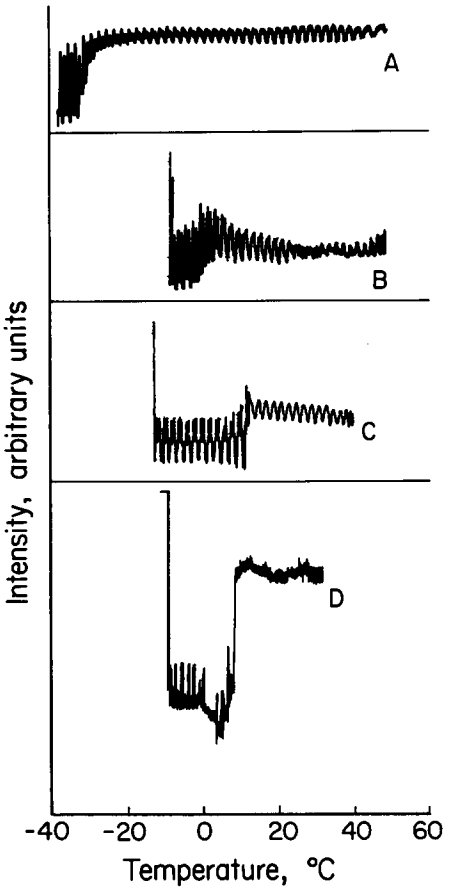

Figure 4 Relative intensity of light backscattered from solution *versus* temperature; PCA data of liquid–liquid phase separation and gelation for (a) 5% PBLGL in 1,2-dichloroethane; (b) 1% PBLG in benzene; (c) 1% PBLG in dioxane/isopropyl alcohol (70/30); (d) 2.0% PBLG in dioxane/water (93.1/6.9)

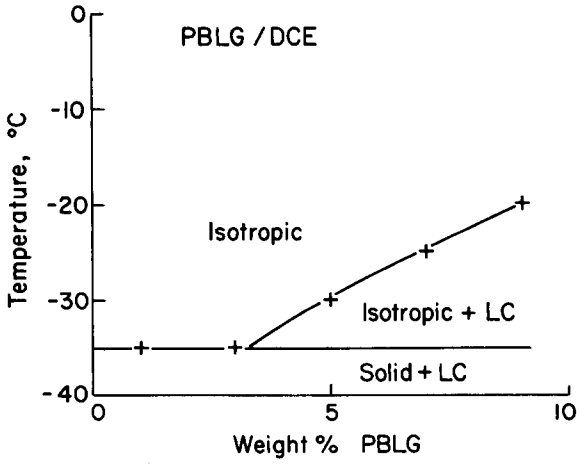

Figure 5 Phase diagram of PBLGL ($M_v=6.6\times10^4$) in 1,2-dichloroethane

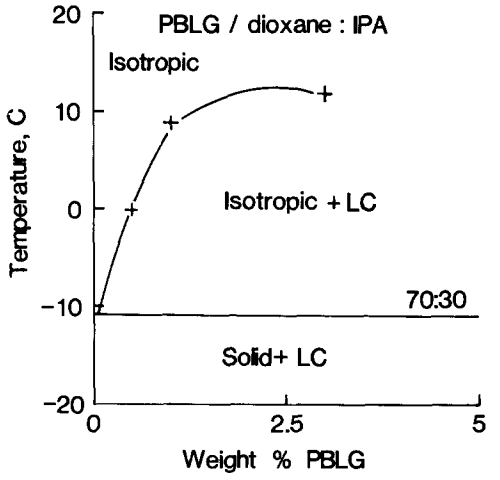

Figure 6 Pseudobinary phase diagram of PBLG ($M_v = 1.9 \times 10^5$) in dioxane/isopropyl alcohol (70/30)

Various cosolvent systems were prepared from dioxane solutions of PBLG (which do not phase separate prior to solvent freezing, as discussed in the later section on liquid–solid phase separation). The cosolvent added was either alcohol or water, which lowers the freezing point of the solution and raises the critical point, exposing the liquid–liquid transition. Dioxane was chosen for the primary solvent because the polymer dissolves more readily in this sublimable solvent than in benzene. In addition, many polar non-solvents for the polymer are miscible with dioxane, allowing the solubility of the polymer to be tailored. The addition of a polar non-solvent also significantly lowers the viscosity of the solution due to disruption of hydrogen bonding responsible for aggregation[12]. This feature makes these very viscous rigid-rod polymer solutions much easier to work with. For example, the value of $|\eta|^*$ for a 2% PBLG solution in dioxane/water is 0.1 Pa s compared to a value of 2 Pa s for a similar concentration of polymer in pure dioxane[25]. The polymer/cosolvent systems studied in this work have been treated as pseudobinary for simplicity, although differential solvent partitioning and alteration of the phase diagram may occur in ternary systems[35]. Although not specifically studied in this work, no differences were observed which were traced solely to the use of a cosolvent system.

The pseudobinary phase diagram for PBLG in a 70/30 mixture of dioxane/isopropyl alcohol is shown in *Figure 6*. A 5% PBLG solution was also prepared at an elevated temperature of 70°C, but could not be made homogeneous. Similar solutions in a 90/10 mixture of dioxane/isopropyl alcohol were prepared but showed no evidence of a liquid—liquid transition prior to solvent freezing, as discussed in the section on liquid–solid phase separation.

Solutions of PBLG in dioxane/water behaved similarly to the dioxane/isopropyl alcohol system, except that much less water was required to raise the critical point. This suggests that water is a stronger non-solvent for PBLG. A pseudobinary phase diagram for PBLG in dioxane/ water mixtures is shown in *Figure 7*. Significant elevation of the cloud point above the freezing point was first detected at 3% water content. Between 5 and 7% water, a shift in cloud point was observed and this shift became more dramatic between 7 and 7.5% water. With increasing water content, homogeneous, high concentration PBLG solutions are difficult to prepare. Therefore, the cloud point curve terminates at 3% polymer at a 7% water content. Higher polymer concentrations were made but the solutions remained phase separated, even at elevated temperature.

In the quiescent testing done in the cooling bath, all the solutions froze in the range of −10 to −13°C, regardless of water content, while polymer-free dioxane/ water mixtures containing 3, 5 and 7% water froze at −4.5, −6.5 and −9.0°C, respectively. This suggests that the PBLG inhibits the nucleation of the solvent in this ternary system.

Solutions of PBLG in benzene were extremely viscous and difficult to manipulate, thus studies in benzene were limited to low concentrations (0.25–1.0%). The solutions in this range of concentrations all showed phase separation 3–5°C above the freezing point of the solution, as shown for the 1% solution in *Figure 4b*. The freezing point is indicated by the sharp rise in intensity at about −12°C.

Rheological measurements during gelation

During the phase equilibria studies in this work, gelation was often observed at, or slightly below, the cloud point; the solutions no longer flowed on inversion of the tube or the oscillation in the backscattered light intensity increased significantly in the PCA, as was shown in *Figure 4*. Gelation has been previously reported for PBLG in dimethylformamide[17,18], toluene[17,18] and benzyl alcohol[20–22]. Rheological studies were used for some of these reports, and we have similarly applied mechanical techniques to verify gelation in our system. These studies have revealed some unique melting behaviour, which may be related to the morphology of the gel.

The dynamic storage moduli, G', for the solution of 1% PBLG in benzene are shown in *Figure 8* in both cooling and heating cycles. Very slow rates (0.25°C/min) were used and a hysteresis of approximately 25°C was observed. The two-stage drop in the modulus response upon heating was very reproducible. After the first decrease in G' at about 27°C, a slight increase was detected. The gel finally melted at about 32°C. An almost

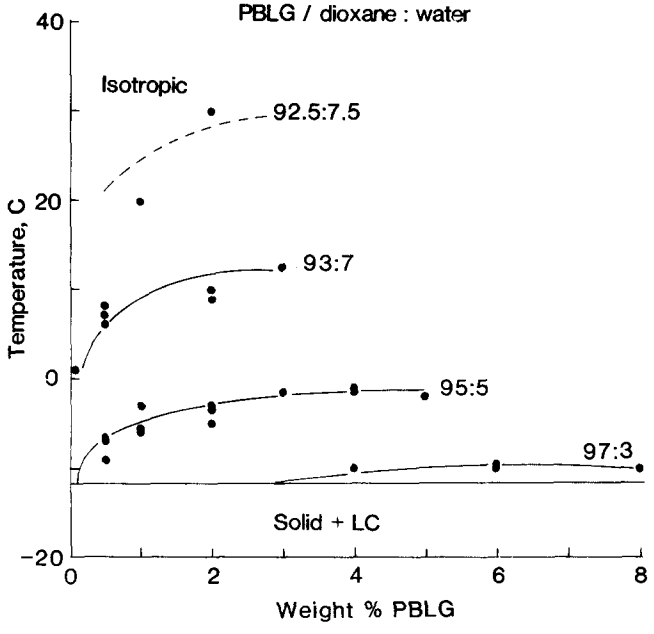

Figure 7 Pseudobinary phase diagram of PBLG ($M_v = 1.9 \times 10^5$) in dioxane/water

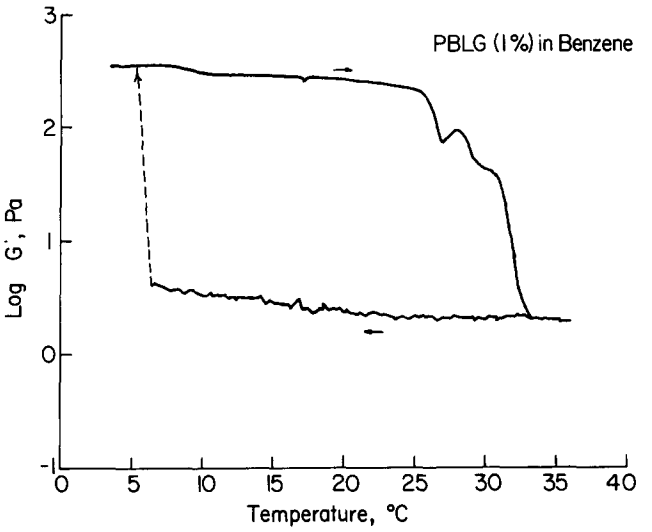

Figure 8 Dynamic shear modulus *versus* temperature for 1% PBLG in benzene at a cooling/heating rate of 0.25°C/min, 1% strain, and 1 Hz

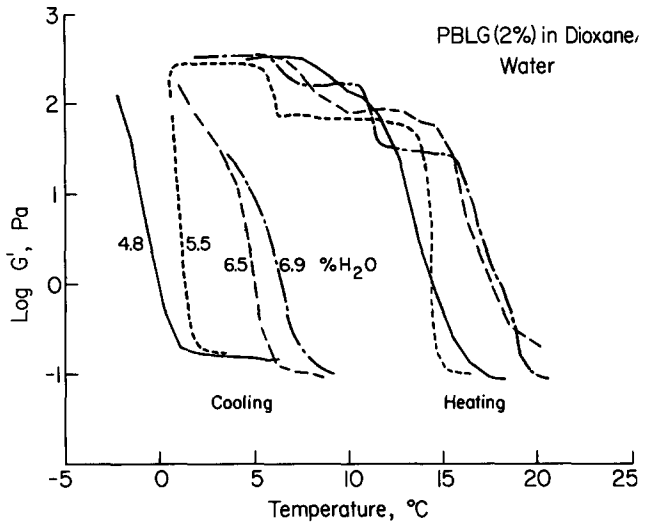

Figure 9 Dynamic shear modulus *versus* temperature for 2% PBLG in dioxane/water at a cooling/heating rate of 0.25°C/min, 1–3% strain, and 1 Hz

identical curve was obtained for a 0.5% PBLG solution in benzene. A gelatin solution subjected to a similar thermal cycle did not exhibit this behaviour[25]. Thus, the two-stage behaviour is not an artifact of the experimental arrangement.

Cooling and heating curves for 2.0% PBLG solutions in dioxane/water mixtures are shown together in *Figure 9*. G' is plotted for four different water concentrations (4.8, 5.5, 6.5, 6.9%). On cooling, the solutions containing greater amounts of water gelled at higher temperatures, which corresponds to the order of the cloud point temperatures. The gels containing higher amounts of water also melted at higher temperatures. Thus, all the PBLG/dioxane/water gels exhibited about 14°C of hysteresis. A two-stage melting was observed for the three lowest water concentrations, while a three-stage melting was observed for the 6.9% water containing solution, to be discussed. Because the cloud points could not be measured simultaneously in the rheometer, comparisons to quiescent cloud points were made. All the gel formation, melting and quiescent cloud point temperatures are summarized in *Figure 10*. The cloud points and gelation temperatures, both obtained on cooling, are in reasonable agreement, which reinforces the PCA observations discussed previously (*Figure 4*).

For the two stages of melting observed for the PBLG gels containing 4.8, 5.5 and 6.5% water, the first decrease in the modulus may be attributed to either the first stage of gel melting or solvent melting (the gelation point is so close to the freezing point that it is difficult to prevent some freezing from occurring). A mixture of dioxane/water (93/7) using the same cooling/heating cycle, froze at 1°C and melted at 5°C. Thus, up to 4°C of hysteresis may be due to delayed nucleation of the solvent crystals on cooling.

In the PBLG solution in dioxane/water (93.1/6.9), a distinct two-stage melting of the gel is observed between 10–20°C, similar to that for the PBLG/benzene solutions. A total of three stages is thus observed, if the decrease at 6°C due to melting of the dioxane/water solvent mixture, discussed above, is included. The first decrease in the modulus of the gel occurred at about 11°C, and the second decrease between 16 and 19°C. The slight increase in modulus observed in the benzene gels after the initial melting was not observed in the dioxane/water gels. Each melting transition for the gels in both solvent systems was quite sharp, occurring over a 1–3°C interval. The larger hysteresis for the 1% PBLG gel in benzene (25°C), compared with the 2% PBLG gel in dioxane/water (14°C), was probably due to the greater hydrogen bonding and aggregation in benzene. In addition, interactions or stacking between the benzyl side chains of PBLG and the benzene molecules may have occurred[11].

A review of the literature of thermoreversible gelation revealed a limited number of papers reporting a two-stage melting of gel structures. Hill and Donald[21,22] observed a suggestion of a two-stage decrease in the rigidity modulus and two d.s.c. endotherms on heating the gels of 10% PBLG in benzyl alcohol. The 10% gel was reported to be initially clear but developed turbidity within a day. Lowering the PBLG concentration to 5% PBLG eliminated the two-stage melting; gels at this concentration were also reported to be clear. Sasaki and coworkers[20] also studied the temperature–modulus response of 0.1–8% PBLG in benzyl alcohol and observed only one-stage melting at these concentrations. Both groups suggested that crystal–solvate formation was responsible for the gel structure. Hill and Donald stated that there is no evidence to connect the sol–gel transition

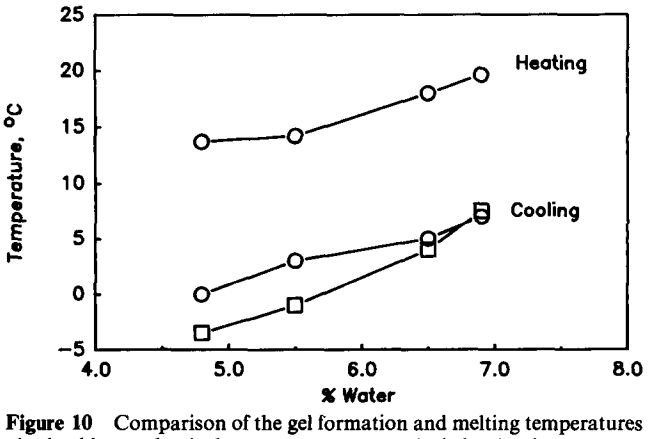

Figure 10 Comparison of the gel formation and melting temperatures obtained by mechanical measurements to optical cloud point temperatures for 2.0% PBLG in dioxane/water. ○, Mechanical; □, optical

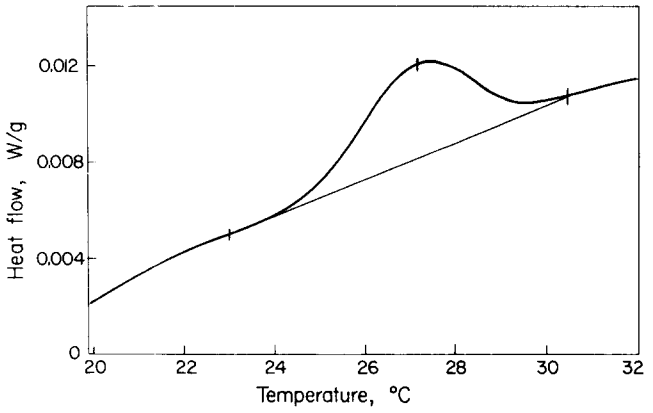

Figure 11 D.s.c. of 1% PBLG in benzene at a heating rate of 5°C/min. Solution cooled rapidly from room temperature and annealed at 6°C for 60 min (sample weight = 39.3 mg)

with entry into the wide biphasic region predicted by Flory, but that it may occur coincidentally, as in the case of the 10% gel. They hypothesized that the two-stage melting of the 10% gels may be a result of a solid LC phase, in addition to the crystal–solvate complex.

Another example of two-stage gel melting is for a flexible polymer rather than a rigid-rod polymer, suggesting a more universal mechanism. Gallego and coworkers[36] examined poly(vinyl chloride) gels in dioctylphthalate at 20–50% polymer. This system has been considered to form a phase separated system[36,37], and also exhibits a two-stage decrease in the modulus–temperature response. The authors interpret the lower transition temperature as the point at which a two-phase gel transforms into a one-phase gel. (This is in accord with the hypothesis by Kawanashi *et al.*[23] that gelation is induced by phase separation into polymer-rich and polymer-poor regions.) However, Gallego does not illustrate how this transformation will influence the shape of the modulus–temperature response. One possibility is that vitrification of the polymer-rich phase would produce an observable glass transition temperature, in addition to the gel melting transition.

The hypothesis that two-stage melting is related to a coincidence of phase separation and gelation is in accord with our observations of PBLG gels in dioxane/water mixtures and in benzene. The gel structure must be formed from the polymer-rich phase, which may subsequently vitrify, crystallize into a solid crystalline phase, or form a solid solution (crystal–solvate). If vitrification were occurring in the polymer-rich phase of the phase-separated solutions and the first modulus drop were a glass transition, then PBLG solutions which do not phase separate before gelling should exhibit a one-stage melting, as the T_g of the gel would be exceedingly low. The clear gels reported for PBLG in benzyl alcohol[20–22] at low concentrations ($\leqslant 5\%$) are an example, although we did not study this system in our rheometer. The behaviour we observed at lower water concentrations of the dioxane/water mixtures (e.g. 95.5/4.8) approaches one-stage melting, and may be another example in which gelation precedes phase separation. However, conclusions are difficult to make due to the additional complication of solvent freezing in this system.

The identification of a solid crystalline phase or a crystal–solvate phase is best accomplished by X-ray diffraction or d.s.c. Although both of these techniques are difficult at the low polymer concentrations studied, a single d.s.c. endotherm at $\approx 27°C$ was observed for the gels formed by 1–10% PBLG in benzene, as shown in *Figure 11*. This melting temperature is in agreement with the value obtained in the rheometer, and confirms that the gel has a crystalline nature. The d.s.c. result does not allow a distinction between a solid crystalline or crystal–solvate phase. However, the latter is more likely due to the low melting point of the gels relative to pure PBLG ($\geqslant 325°C$).

Another possible explanation for the two-stage melting is based on the observed foam morphology for the PBLG in benzene and dioxane/water (93/7) solution. At slow cooling rates, the fibrous structures which formed were distinctly bimodal in fibre diameter. It is conceivable that the two-stages are due to this feature, with the small fibres melting first. The possible origin of the bimodal morphology will be discussed later.

Liquid–solid phase separation

Solutions of PBLG in dioxane (0.5–14%), 1,4-dichlorobenzene (1–7%), naphthalene (1–7%) and dioxane/isopropyl alcohol (90/10) (1–7%) showed no evidence of liquid–liquid phase separation prior to solvent freezing. Solutions in naphthalene and 1,4-dichlorobenzene were extremely viscous and difficult to dissolve, even at elevated temperature. It is possible that liquid–liquid phase separation would be difficult to observe for the naphthalene solution because the refractive indices of naphthalene (1.5898) and PBLG[38] (1.59–1.60) are very close. The concentration of PBLG solutions in dioxane extended into the narrow biphasic region, as verified by birefringence observed in a polarizing microscope. The absence of liquid–liquid phase separation prior to solvent freezing in dioxane is in agreement with the remarks of Toyoshima and coworkers[39].

Foam formation and characterization

Conditions of foam formation. The foams were prepared by rapidly cooling solutions of PBLG in various solvents until the solution was completely frozen, and then removing the solvent by vacuum sublimation. In most cases, liquid nitrogen was used as the cooling medium and a uniaxial quench was applied using the foam mould design shown in *Figure 2*. This simplifies the interpretation of the morphologies obtained, and produces more defect free foams[3]. Other cooling rates and mould designs were used in the cases specified.

Morphology. The foam morphologies produced by liquid–solid phase separation were generally larger in scale and of less interest than those produced by liquid–liquid phase separation. However, a brief summary of the structures produced by liquid–solid phase separation will be given first to help clarify the rest of the discussion.

The liquid–solid phase separation of PBLG in pure dioxane produced three different foam morphologies, depending on the concentration of the solution, cooling rate and cooling direction, as shown in *Figure 12*. Rapid uniaxial cooling produced an anisotropic ladder-like (*Figure 12a*) or sheet-like (*Figure 12b*) structure, where the long axes of the ladders or sheets are parallel to the direction of cooling. This suggests that the polymer is pushed to the grain boundaries by the advancing solvent crystal front. The ladder-like structure was favoured for

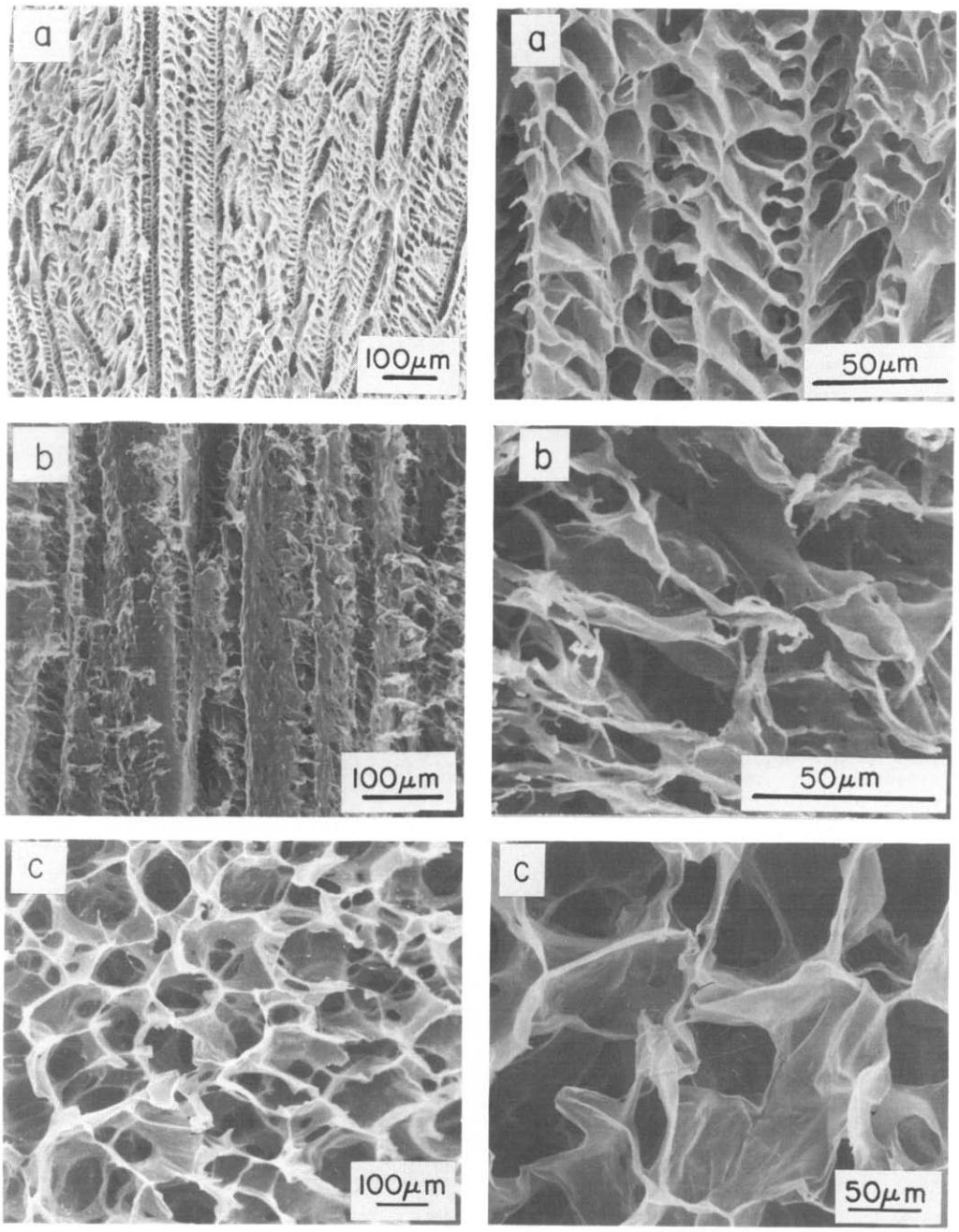

Figure 12 Liquid–solid phase separation: SEM of foams from dioxane solutions (a) 5% PBLGL in a uniaxial quench (vertical) produces an anisotropic, ladder-like morphology; (b) 2% PBLG in a uniaxial quench (vertical) produces an anisotropic, sheet-like morphology; (c) 1.0% PBLG in slow cooling produces an isotropic, large-cell morphology

higher concentration solutions and faster quench rates. The inability of the polymer to diffuse out of the path of the impinging solvent crystals may have caused the regularly spaced ladders. The sheet-like morphology is similar to structures reported for the polystyrene/benzene system[3], where liquid–liquid phase separation does not occur. The isotropic morphology produced by slow cooling is shown in *Figure 12c*, and is indicative of random solvent crystallization throughout the solution. In this case, an interconnected, closed cell structure with cell diameters of $\approx 100\,\mu m$ was formed.

It is also significant to note that no differences were observed in the morphology of foams prepared from the narrow biphasic region of the phase diagram for PBLGL in dioxane (11–14%). Thus, the simple coexistence of isotropic and LC phases does not produce any unique morphology, under the rapid uniaxial cooling conditions used. In addition, the cosolvent system dioxane/isopropyl alcohol (90/10) also produced foams with similar morphology to those shown in *Figure 12*.

The morphology produced by liquid–liquid phase separation and gelation of PBLG in solution will be discussed next. Foams of PBLG formed after a liquid–liquid phase separation in the cosolvent system dioxane/water proved to be the most amenable to study, due to the ease of sublimation processing at low water concentrations (< 10%). Addition of 3–5% water caused a lacy microcellular morphology to emerge on the walls of the ladder-like or sheet-like morphology obtained from pure dioxane solutions. *Figure 13* illustrates this combined morphology at × 1200. The fibrous morphology, which is believed to be due to phase separation and gelation, is

superimposed on the larger scale structure hypothesized to form via solvent freezing.

At slightly higher water concentrations (i.e. 7%), a structure was produced which showed no evidence of directionality due to solvent freezing. This unique morphology is shown in *Figure 14* for a 2% PBLG foam. The magnifications illustrated are $\times 1000$ and $\times 5000$, ten times those of *Figure 12* for the morphologies obtained from liquid–solid phase separation. The fibrous, interconnected structure was uniform over the entire cross section. Similar morphology was obtained from 1% and 3% PBLG solutions. The fibre-like foams were much tougher than the coarser foams and almost impossible to cut by hand with a blade without crushing the foam. The vibrating microtome blade was essential for producing a flat surface for SEM examination of these foams.

The fibrous struts shown in *Figure 14* have a very smooth surface appearance. This is in contrast to the highly twisted 'super-helical' fibrils observed by transmission electron microscopy of precipitates of PBLG[15,16], formed either by mixing a solution of polymer with a strong acid, or by very prolonged ageing of the gels. It is not known at this time what factors determine whether the fibres are smooth or twisted, but the initial solution concentration and method of preparation are clearly influential.

Quench-rate has been reported to affect the mechanism by which the microcellular structure forms[3,5,6] in both non-gelling[3] and gelling[6] solutions, and was studied for the dioxane/water system. For the 1–3% PBLG foams from the solution of dioxane/water (93/7), some differences in the morphology were observed for the conventional uniaxial quench using liquid nitrogen (cooling rate of ≈ 100°C/min). At the bottom (highest quench rate), uniform fibre diameters ($\approx 1\ \mu$m) were observed. At the top (lowest quench rate), a bimodal distribution of fibre diameters was present (≈ 0.2 and $\approx 1\ \mu$m) and the cell structure was much finer in some regions but less homogeneous. This is different from the coarsening behaviour reported for the non-gelling system of polystyrene in cyclohexane[3], in a uniaxial quench.

Two solutions were chosen for the quench-rate study: 2.0% PBLG in dioxane/water (95/5); and 2.0% PBLG in dioxane/water (93/7). The difference between the cloud point and the quiescent freezing point was ≈ 7°C for the 95/5 solution and ≈ 19°C for the 93/7 solution. (This difference may actually be less, as the freezing points determined in the dynamic gelation experiments were higher, perhaps due to the slight agitation provided.) Five different cooling modes were investigated:

Mode 1 Liquid nitrogen
Mode 2 Dry ice/acetone
Mode 3 Fast to cloud point/fast to freezing point
Mode 4 Slow to cloud point/fast to freezing point
Mode 5 Slow to cloud point and freezing point

Here the 'fast' rate was achieved by direct quenches, whereas the 'slow' rate was controlled at 0.2°C/min. The solutions containing a cosolvent ratio of dioxane/water (95/5), yielded a combination of morphologies from both solvent freezing and liquid–liquid phase separation, regardless of the cooling rate. An SEM micrograph illustrating this structure was given in *Figure 13*. The fibre-like morphology, which is believed to be a product of liquid–liquid phase separation, is superimposed on a larger scale morphology produced by solvent freezing. This larger scale structure takes three different forms, as previously discussed for liquid–solid phase separation in pure dioxane. A ladder-like morphology was produced at the fastest cooling rate (Mode 1), a sheet-like morphology was produced with more moderate rates (Mode 2), and a large-cell isotropic morphology was produced at slow cooling rates (Modes 4 and 5). The observation that the ladder-like structure is favoured over

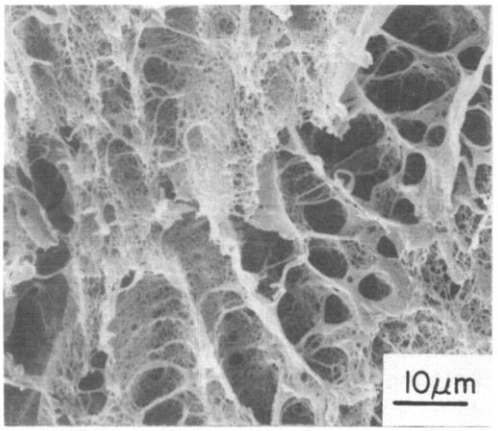

Figure 13 Combination of morphology from liquid–solid and liquid–liquid phase separation in a uniaxial quench (vertical): SEM of foam from 2.0% PBLG in dioxane/water (95/5)

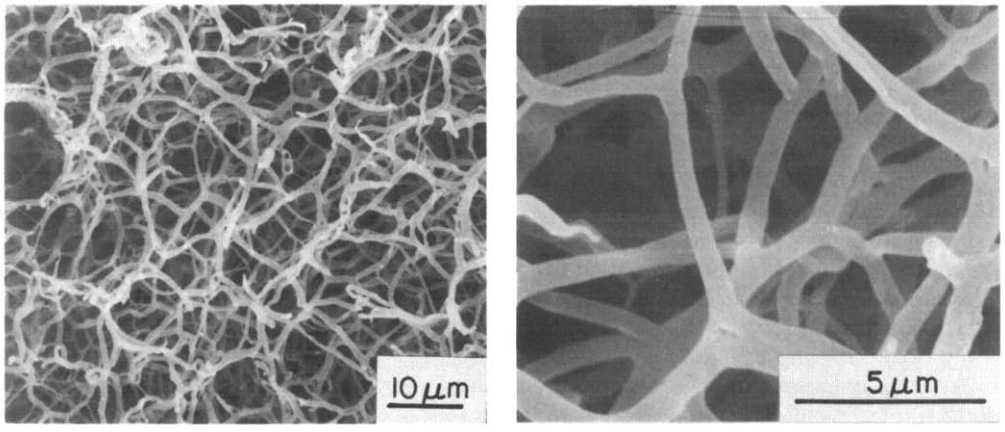

Figure 14 Liquid–liquid phase separation: SEM of foam from 2.0% PBLG in dioxane/water (93/7) in a uniaxial quench shows a uniform three-dimensional fibre-like morphology

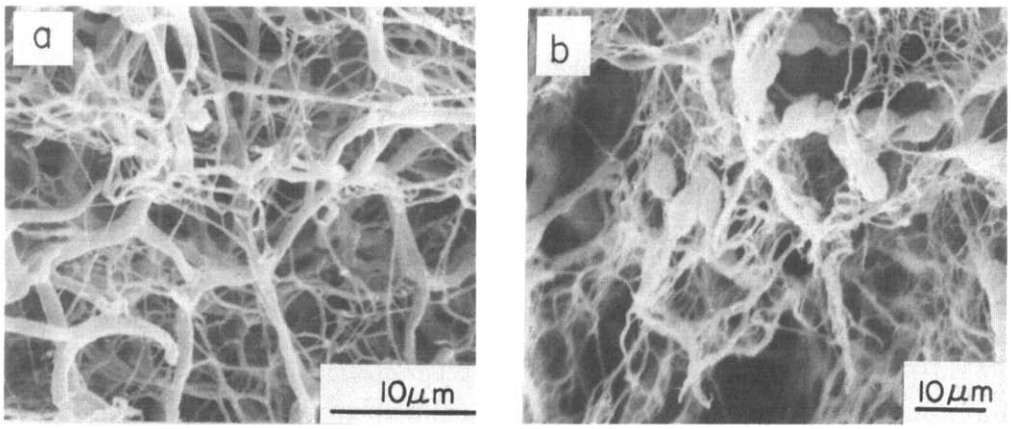

Figure 15 SEM of foams from 2.0% PBLG in dioxane/water (93/7) at slower cooling rates showing formation of interconnected fibres of different diameters (a) cooling rate ~5°C/min; (b) cooling rate of ~0.2°C/min or slower

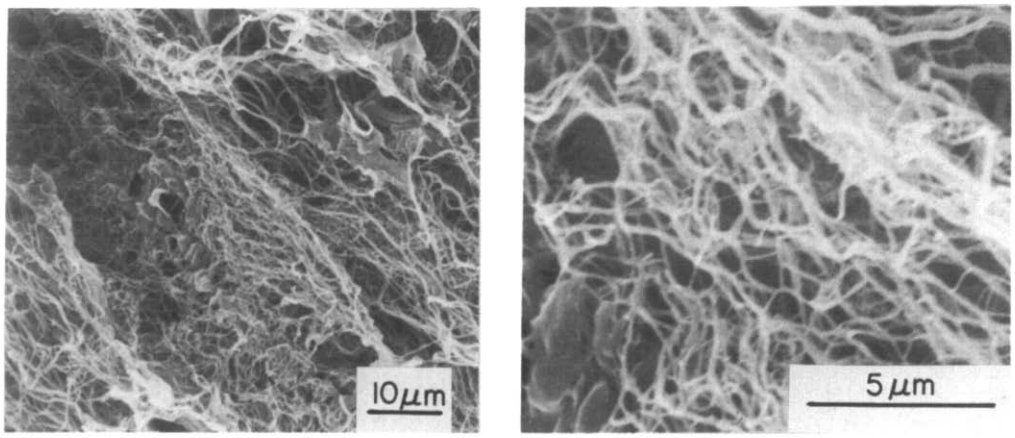

Figure 16 Liquid–liquid phase separation: SEM of foam from 0.25% PBLG in benzene in a uniaxial quench shows a three-dimensional fibre-like morphology

the sheet-like structure at higher quench rates supports the hypothesis that it is due to a high solution viscosity and low polymer diffusion rate relative to the rate of solvent crystallization.

The solutions containing a cosolvent ratio of dioxane/water (93/7) gave continuous fibre-like structures for all modes of cooling. All the foams did not crumble and were tenacious during cutting. Thin slices of the foams were easily stretched. The bimodality of fibre diameters became more pronounced at slower cooling rates (Mode 3 and higher). An example is given in *Figure 15a*. Very large agglomerates of fibres were present for Mode 5, where groups of the small diameter fibres have twisted together into a bundle, as illustrated in *Figure 15b*. These were not formed during the cutting of the sample, for a broken surface of the foam exhibited the same morphology. The primary difference between Mode 4 and Mode 5 was that large holes were present for Mode 5 where the solvent nucleated and crystallized due to the slow rate of cooling during the freezing process. This effect was discussed above for the 95/5 solutions.

In summary, the results for the dioxane/water (95/5) solutions are much more difficult to interpret than those for the dioxane/water (93/7) solutions, which gave a fibre-like morphology at all cooling rates. The complication of solvent freezing in combination with phase separation and gelation is believed to be responsible. If the phase separation process is immobilized by gelation and cannot be completed, a uniform fibre structure may not develop before the solvent begins to freeze. This explains why a morphology similar to the 93/7 solution was never obtained, even at slow cooling rates. For the 95/5 solutions, gelation was observed in quiescent experiments at or below the cloud point, and in the rheological studies, gelation and freezing were almost coincident for the 95.2/4.8 solution.

Foams prepared from benzene solutions in a uniaxial quench in liquid nitrogen featured a similar interconnected fibre-like structure, shown in *Figure 16*. The fibre diameters showed a bimodal nature. A large amount of shrinkage (>400%) occurred for this particular form, which was prepared from a very dilute solution (0.25%). This may explain the less uniform network compared to foams prepared from dioxane/water (93/7). Although the concentrations studied in benzene were limited, foams made at 1% polymer in solution for both benzene and dioxane/water (93/7) gave a similar bimodal morphology at slow cooling rates, which is a useful example that this morphology cannot simply be ascribed to the use of a cosolvent system.

A number of hypotheses might explain the coexistence of distinctly fine (0.2 μm) and coarse (1–2 μm) fibre diameters in foams from both dioxane/water (93/7) and benzene solution, illustrated in *Figures 15* and *16*, respectively. The existence of two mechanisms, or two-stages of the same mechanism, might be responsible. For example, in a uniaxial quench, phase separation may precede gelation at the faster cooling rates at the bottom

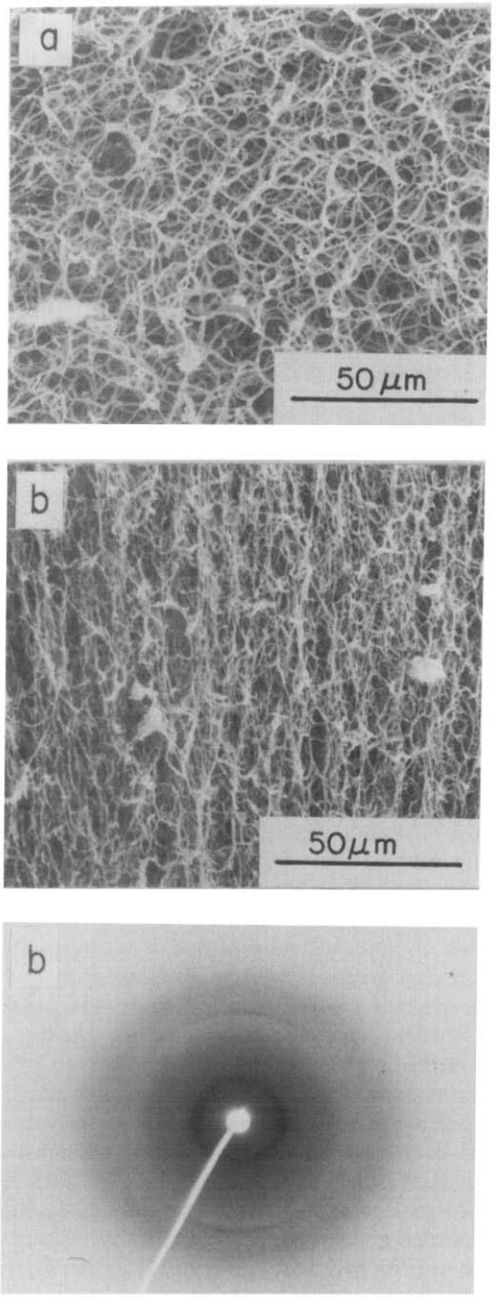

Figure 17 SEM and X-ray diffraction of fibre-like foam from 2.0% PBLG in dioxane/water which has been stretched shows preferred orientation in the direction of stretch (vertical) (a) unstretched; (b) stretched

of the sample. If gelation later begins at the top of the sample, the finer fibres observed there may be a remnant of the gel. Another possible explanation is the concurrence of heterogeneous and homogeneous nucleation processes. Alternatively, a combination of early and late stage structures from the same mechanism could also produce structures with the appearance of bimodality. More work is necessary to elucidate the origin of this bimodality.

Crystalline orientation of 'fibres'. SEM and X-ray diffraction studies were conducted on thin slices (0.5–1.0 mm) of the fibre-like foams formed from 2.0% PBLG in dioxane/water (93/7). The SEM micrographs of the unstretched and stretched foams, shown in *Figure 17a* and *b*, respectively, demonstrate that the struts were oriented in the direction of stretch (vertical). The WAXS studies of the stretched fibre structure showed that a preferred orientation was produced by stretching as shown in *Figure 17b* (manifested as arcs for the stretched samples *versus* rings for the unstretched). Meridional arcs corresponding to the helical pitch (5.2 Å) and equatorial arcs corresponding to the interrod spacing (13.5 Å), of PBLG[40] were observed, which suggests that the crystals of the polymer are parallel to the fibre axes. The unknown factor in stretching the foam is whether the struts were simply being oriented or whether the polymer in the struts was additionally drawn out like a fibre. If the latter is the case, a more definitive technique is necessary, such as electron diffraction of an individual strut.

Thin slices of the foam made from PBLG in pure dioxane (anisotropic, sheet-like morphology) did not stretch but tore easily. SEM and X-ray diffraction studies were not possible for a stretched foam of this sample.

PBLG is a highly crystalline polymer in the solid state and thus birefringent under crossed polarizers in the optical microscope. If preferred orientation were present relative to the strut axes, the struts would exhibit extinction at a 90° rotation of the microscope stage. This would be very difficult to observe, however, if the aligned regions were small. If the slow direction of the strut can be determined, the placement of the rods parallel or perpendicular to the strut axis can be ascertained.

Each of the two foams discussed above (ladder-like and fibre-like) were embedded with an epoxy matrix to section for optical microscopy. A photomicrograph of the embedded fibrous structures is shown in *Figure 18*, and appears as a mesh-like grid, with maximum brightness at a position of 45° between crossed polarizers. Because more than one layer was present, the entire sample was not in focus at high magnification. The individual struts could be distinguished at × 1000 and exhibited fibre-like extinction when the stage was rotated. This indicates that the PBLG rods in this foam were oriented in the individual struts. The sign of the birefringence of the polymer crystals which comprised the struts was positive, indicating that the orientation of the molecules was parallel to the strut axes.

Drawn fibres of PBLG and other lyotropic LCPs have been reported to form closely packed bright bands at right angles to the fibre axis, when the fibre axis is parallel to either the polarizer or analyser under complete extinction conditions[41]. No such bands were observed in the embedded foams of PBLG; however, the fibre diameters in the foam are only 0.2 to 2 μm, much smaller than the 20–30 μm diameters produced by drawing. If banded structures were present, they were beyond the resolution of the optical microscope.

Optical microscopy of the embedded ladder-like foam showed a much coarser and less homogeneous structure compared to the fibre-like foam. Because this foam was anisotropic and the position of the cut through the sample was not known (i.e. parallel to the 'ladder' or otherwise), it was impossible to coordinate any fibre-like extinction to the actual form morphology. Extinction was observed in some regions, and the sign of the birefringence was also positive.

Mechanical properties. The moduli obtained for PBLG and PS foams produced by liquid–liquid phase separation were compared with the micromechanical model developed by Warren and Kraynik[42]. This model assumes

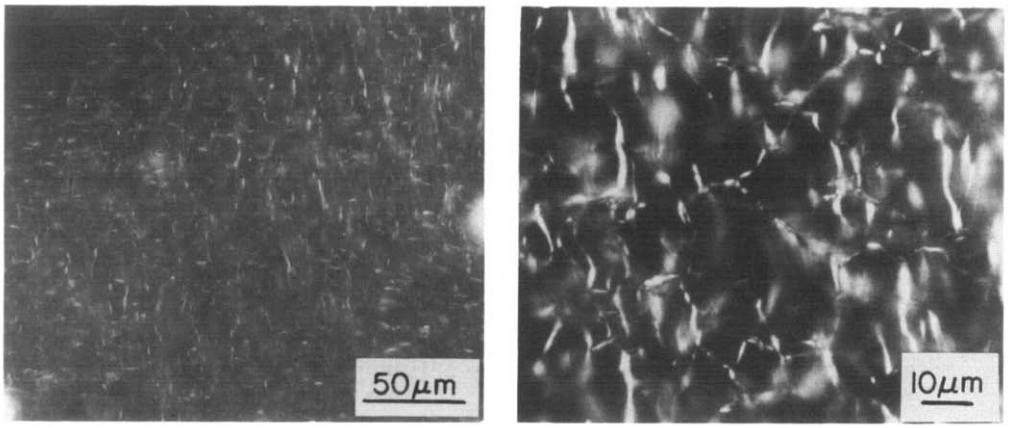

Figure 18 Optical micrograph of epoxy embedded foam with fibre-like morphology from 2.0% PBLG in dioxane/water (93/7) under crossed polarizers

Table 1 Comparison of experimental and theoretical foam moduli

Polymer	ϕ	E_f (MPa) Experimental (22°C)	E_f (MPa) Predicted[a]
Polystyrene	0.039	1.1±0.1[b]	2.8
Polystyrene	0.122	13±1	27
PBLG	0.031	2.0±0.2	1.1

[a] Using a value of $E_s = 2000$ MPa for PS and 1300 MPa for PBLG at 22°C, as described in Reference 26
[b] One standard deviation reported

that the foam is of low density and that the strains are small, resulting in bending as the primary mode of deformation. For circular strut cross sections, assumed to be the most probable for these foams, this model predicts:

$$E_f/E_s = 0.91\phi^2 \quad (1)$$

In this equation, E_f and E_s are the modulus of the foam and polymer, respectively, and ϕ is the volume fraction of polymer (simply the foam density divided by the polymer density).

The experimentally determined values[26] for PBLG and PS are given in *Table 1*, and compared with the values predicted by equation (1). This comparison is somewhat subjective since the precise value of E_s is not known, as discussed elsewhere[26]. The moduli of the PBLG foams were slightly dependent on frequency in the temperature range of 15 to 30°C. This can be explained in terms of a side-chain motion for PBLG at around room temperature[43]. The polystyrene foam modulus was independent of temperature in this range. Critical testing of this theory requires analysis of foams of different types with a broader range of densities, and is presented elsewhere[26].

Discussion of the mechanism of liquid–liquid phase separation

One of the original tenets of this work was that foam structure may be indirectly used to study the liquid–liquid phase separation process. Previous work has shown that for dilute solutions of amorphous random-coil polymers, rapid quenching is required to produce an interconnected foam structure. For this reason, the mechanism of phase separation has been suggested to be spinodal decomposition rather than nucleation and growth[2,3]. For semi-crystalline polymers, which can form gel structures, microcellular materials have been produced with slow cooling[5,6].

We have emphasized the study of foams prepared from <3% PBLG solutions, well below the concentration at which the isotropic to liquid crystal transition is predicted[29] to occur. The Flory theory as it relates to an isotropic solution of rods brought into the wide biphasic region is thus of primary concern, as discussed in the first section of the Results. The dynamics of phase separation in such a system is difficult to predict and the behaviour of the spinodal, especially in the region of concentration around v_2^* and below, is unclear due to limitations of the theory. However, if the theory is strictly adhered to, namely, the disordered free energy function is valid in the isotropic region and the spinodal is the second derivative of this function, a rather large gap exists between the binodal and the spinodal curves at low polymer concentrations.

The foam morphology obtained by liquid–liquid phase separation from both benzene and dioxane/water solution was a highly interconnected fibre-like structure. This interconnected morphology was formed at both fast and slow cooling rates, and was found to be associated with thermoreversible gelation at or below the cloud point. However, the final foam morphology must also reflect late-stage processes, and it is known that both mechanisms of phase separation may lead to similar final morphologies under some circumstances[44]. Thus, this discussion is speculative, as the direct kinetic studies of the dynamics of phase separation were limited. (Preliminary temperature-jump light scattering experiments showed no evidence of a 'spinodal ring'[25]. However, time constraints and instrumental difficulties made these results inconclusive.)

If nucleation for these rod-like molecules were very slow due to the high degree of order necessary to nucleate the LC phase[45], leisurely cooling into the unstable spinodal region would be feasible. The interconnected fibre-like structures observed do seem reminiscent of a continuous spinodal process. It is normally believed unlikely that nucleated polymer phase could interconnect in such a fashion, unless the growth of the LC phase were very dendritic. A model proposed for the formation of networks of rod-like polymers by Uematsu and Uematsu[11] shows the branching and rejoining of different sheaf-like aggregates to produce fibrillar structures. The rod axes are parallel to the fibre axes in this model. They do not specify whether nucleation and

growth or spinodal decomposition is the mechanism. However, the one-dimensional diffusion model of rods from an oriented solution developed by Cohen and Thomas[19] predicts a fibrillar morphology for nucleation and growth and a lamellar morphology for spinodal decomposition. This suggests that the structure proposed by Uematsu would be formed via a nucleation and growth mechanism. Doi and Kuzuu[46] considered the structure of the interface between the nematic and isotropic phase in rod-like molecules, based on surface tension arguments. They predicted that parallel alignment of the rods to the interface would be energetically more stable than perpendicular alignment. This prediction also supports the Uematsu structure.

The experimental evidence obtained in this work supports the Uematsu model, based on the positive sign of birefringence observed for the fibres which comprise the foam struts. If this structure were formed by a nucleation and growth mechanism, as predicted by the model of Cohen and Thomas, then this is the most likely mechanism for the formation of foams by this process. Other supporting evidence includes the insensitivity to cooling rate, the lack of a 'spinodal ring' in light scattering studies and the evidence that supercooling occurred in some solutions. The calculation of the spinodal made for the Flory theory of rod-like particles, if strictly followed, also suggests difficulty in reaching the spinodal region from the very dilute solutions studied in this work.

CONCLUSIONS

The main goals of this research were to study the phase behaviour and gelation of solutions of LCPs and prepare microcellular foams by thermally induced phase separation processes. The model polymer used in this work was PBLG. The study of both liquid–solid and liquid–liquid phase separation both in single and two component solvent systems was achieved. No differences were observed which could be solely traced to the use of a cosolvent system. The solvents chosen could be successfully removed by vacuum sublimation of the frozen solutions. Foam densities in the range of 0.015–0.06 g/cm^3 were studied the most extensively, as an emphasis was placed on low density materials.

Liquid–solid phase separation of PBLG solutions produced a ladder-like or sheet-like morphology in a uniaxial quench, indicative of solvent crystallization. The long axis of the 'ladders' correlated with the direction of cooling. The cell sizes varied from 10–50 μm depending on the quench rate. Faster quench rates produced smaller cell sizes. The ladder-like morphology was favoured over the sheet-like morphology at high concentration and viscosity, and faster cooling rates.

Liquid–liquid phase separation and gelation produced materials with a unique structure and physical properties. The foams resembled a three-dimensional lattice consisting of fibre-like struts with very little wasted polymer material at the junction points. The cell diameters ranged from 1–10 μm while the strut diameters ranged from 0.2–2.0 μm. A bimodal distribution of fibre diameters was observed to form at slower quench rates, possibly due to a combination of two processes occurring simultaneously, or two stages of the same process. It is noteworthy that the fibre-like foams discussed in this work are formed non-mechanically, in contrast to fibres made by conventional drawing or spinning processes.

Gelation was found to play a key role in the liquid–liquid phase separation of these solutions, and was verified by rheological experiments. This is not unexpected, as many reports indicate that PBLG solutions form gels upon entering the wide biphasic region. This is the first report, however, on PBLG gels in benzene and the cosolvent system dioxane/water. The phenomenon of gelation explains why rapid quenching was not necessary to produce the fibre-like morphology. Similar results were reported by Aubert[6] for isotactic polystyrene materials made from gels in nitrobenzene. In fact, the morphology of his dried gels quite closely resembles our PBLG foams (although on a smaller size scale).

The gelation studies produced another significant result: a distinct two-stage melting in the modulus-temperature response of the gel. This has been tentatively assigned to the disappearance of a solid PBLG or a PBLG-rich solid solution, and, at higher temperatures, the dissolution of the continuous LC phase. The possibility also exists, however, that the bimodal fibre diameters observed at slower cooling rates in the foams were also present in the gel, and melted at slightly different temperatures. In the PBLG/benzene system, after the first decrease in modulus at $\approx$27°C, a slight increase was observed before the final melting. This behaviour may be a clue to the nature of these gels, and perhaps new foam materials. The two-stage melting was observed for both solvent systems that yielded the fibre-like foam morphology. Similar reports of the modulus–temperature response of gels made from very dilute solutions (0.5–2.0%) in volatile organic solvents are quite rare.

An argument was given to support a nucleation and growth mechanism of phase separation and gelation, based on experimental evidence obtained and considering various models for rod-like molecules. This discussion is speculative because direct kinetic studies were very limited. It is anticipated that future theoretical and experimental developments of the dynamics of phase separation for rod-like polymers will help resolve these issues.

ACKNOWLEDGEMENTS

We are grateful to Drs J. H. Aubert and J. G. Curro of Sandia National Laboratories, Albuquerque and Professor E. T. Samulski of The University of North Carolina at Chapel Hill, for many helpful discussions. We thank Dr Barbara Poliks for consultation on the spinodal calculations. Appreciation is also expressed to Sandia National Laboratories, Albuquerque and the US Army Research Office for financial support of this research.

REFERENCES

1 Caneba, G. T. and Soong, D. S. *Macromolecules* 1985, **18**, 2538
2 Castro, A. J. US Patent 4 247 498, November 24, 1978
3 Aubert, J. H. and Clough, R. L. *Polymer* 1985, **26**, 2047
4 Young, A. T., Moreno, D. K. and Marsters, R. G. *J. Vac. Sci. Techn.* 1982, **20**, 1094
5 Young, A. T. *J. Cell Plastics* 1987, **23**, 55
6 Aubert, J. H. *Macromolecules* 1988, **21**, 3468
7 Doi, M. and Edwards, S. F. 'The Theory of Polymer Dynamics', Ch. 8–10, Clarendon Press, Oxford, 1986
8 Ying, Q. and Chu, B. *Macromolecules* 1987, **20**, 362
9 Prevorsek, D. C. in 'Polymer Liquid Crystals', (Eds A. Ciferri, W. R. Krigbaum and R. B. Meyer) Academic Press, New York, 1982, Ch. 12

10 Northolt, M. G. in 'Recent Advances in Liquid Crystalline London, 1985, Ch. 20
11 Uematsu, I. and Uematsu, Y. *Adv. Polym. Sci.* 1984, **59**, 37
12 Sakamoto, R. *Coll. Polym. Sci.* 1984, **262**, 788
13 Ciferri, A. in 'Polymer Liquid Crystals', (Eds A. Ciferri, W. R. Krigbaum and R. B. Meyer) Academic Press, New York, 1982, Ch. 3
14 Doty, P., Bradbury, J. H. and Holtzer, A. M. *J. Am. Chem. Soc.* 1956, **78**, 947
15 Ishikawa, S. and Kurita, T. *Biopolymers* 1964, **2**, 381
16 Tachibana, T. and Kambara, H. *Kolloid-Z. Z. Polym.* 1967, **219**, 40
17 Miller, W. G., Kou, L., Tohyama, K. and Voltaggio, V. *J. Polym. Sci., Polym. Symp.* 1978, **65**, 91
18 Russo, P. S., Magestro, P. and Miller, W. G. in 'Reversible Polymeric Gels and Related Systems', (Ed. P. S. Russo) American Chemical Society: Washington DC, (1987), ACS Symp. Ser. No. 350, Ch. 11
19 Cohen, Y. and Thomas, E. L. *Polym. Eng. Sci.* 1985, **25**, 1093
20 Sasaki, S., Hikata, M., Shiraki, C. and Uematsu, I. *Polym. J.* 1982, **14**, 205
21 Hill, A. and Donald, A. M. *Mol. Cryst. Liq. Cryst.* 1987, **153**, 395
22 Hill, A. and Donald, A. M. *Polymer* 1988, **29**, 1426
23 Kawanashi, K., Komatsu, M. and Inoue, T. *Polymer* 1987, **28**, 980
24 Tan, H-M., Moet, A., Hiltner, A. and Baer, E. *Macromolecules* 1983, **16**, 28
25 Jackson, C. L. *PhD Dissertation*, The University of Connecticut, Storrs, CT, 1988
26 Jackson, C. L., Shaw, M. T. and Aubert, J. H. Submitted to *Polymer*
27 Gent, A. N. and Lindley, P. B. *Proc. Inst. Mech. Eng.* 1959. **173**, 111
28 Onsager, L. *Ann. N. Y. Acad. Sci.* 1949, **51**, 627
29 Flory, P. J. *Proc. R. Soc. London, Ser. A* 1956, **234**, 73
30 Odijk, T. *Macromolecules* 1986, **19**, 2313 and references therein
31 Romanko, W. R. and Carr, S. H. *Macromolecules* 1988, **21**, 2243
32 Doi, M., Shimada, T. and Okano, K. *J. Chem. Phys.* 1988, **88**, 4070
33 Wee, E. L. and Miller, W. G. in 'Liquid Crystals and Ordered Fluids', Vol. 3 (Eds J. F. Johnson and R. S. Porter) Plenum, New York, 1978, 371
34 Jackson, C. L., Samulski, E. T. and Shaw, M. T. *PMSE Preprints* 1987, **57**, 107
35 Russo, P. S. and Miller, W. G. *Macromolecules* 1984, **17**, 1324
36 Gallego, F., Muñoz, M. E., Peña, J. J. and Santamaria, A. *J. Polym. Sci., Polym. Phys. Edn.* 1988, **26**, 1871
37 Boo, H. K. and Shaw, M. T. *J. Vinyl Techn.* 1987, **9**, 168
38 Kratohvil, J. P. *Kolloid-Z. Z. Polym.* 1970, **238**, 455
39 Toyoshima, Y., Minami, N. and Sukiga, M. *Mol. Cryst. Liq. Cryst.* 1976, **35**, 325
40 Bamford, C. H., Elliott, A. and Hanby, W. E. 'Synthetic Polypeptides', Academic Press, New York, 1956, 263
41 Horio, M., Ishikawa, S. and Oda, K. *J. Appl. Polym. Sci., Appl. Polym. Symp.* 1985, **41**, 269
42 Warren, W. E. and Kraynik, A. M. *J. Appl. Mech.* 1988, **55**, 341
43 Hiltner, A., Anderson, J. M. and Borkowski, E. *Macromolecules* 1972, **5**, 446
44 McMaster, L. P. *Adv. Chem. Ser.*, (Am. Chem. Soc., Washington DC) 1975, **142**, 43
45 Papkov, S. P. in 'Contemporary Topics in Polymer Science', Vol. 2, (Eds E. M. Pearce and J. R. Schaefgen) Plenum, New York, 1977, 97
46 Doi, M. and Kuzuu, N. *J. Appl. Polym. Sci., Appl. Polym. Symp.* 1985, **41**, 65